Photoinduced Magnetization with a High Curie Temperature and a Large Coercive Field in a Co-W Bimetallic Assembly

*Noriaki Ozaki, Hiroko Tokoro, Yoshiho Hamada, Asuka Namai, Tomoyuki Matsuda, Souhei Kaneko, and Shin-ichi Ohkoshi**

The crystal structure, magnetic properties, and temperature- and photoinduced phase transition of $[\{Co^{II}(4\text{-methylpyridine})(pyrimidine)\}_2\{Co^{II}(H_2O)_2\}\{W^V(CN)_8\}_2]\cdot 4H_2O$ are described. In this compound, a temperature-induced phase transition from the Co^{II} ($S = 3/2$)-NC-W^V($S = 1/2$) [high-temperature (HT)] phase to the Co^{III}($S = 0$)-NC-W^{IV}($S = 0$) [low temperature (LT)] phase is observed due to a charge-transfer-induced spin transition. When the LT phase is irradiated with 785 nm light, ferromagnetism with a high Curie temperature (T_C) of 48 K and a gigantic magnetic coercive field (H_c) of 27 000 Oe are observed. These T_C and H_c values are the highest in photoinduced magnetization systems. The LT phase is optically converted to the photoinduced phase, which has a similar valence state as the HT phase due to the optically induced charge-transfer-induced spin transition.

1. Introduction

In recent years, cyanobridged bimetal assemblies have been aggressively studied to demonstrate various magnetic functionalities, such as room temperature magnetic ordering,[1] thermal phase transition,[2] photoinduced magnetization,[3,4] humidity-induced magnetism,[5] non-linear magneto-optical effects,[6] gas adsorption,[7] and negative (or zero) thermal expansion.[8] In particular, photomagnetism is an attractive issue. One approach to realize optical control of magnetization is to use irradiation to change the electronic spin state of a magnetic material. From this viewpoint, octacyanometalate-based compounds are useful systems for preparing photomagnetic materials because $[M(CN)_8]^{n-}$ (M = Mo, W, Nb, etc.) can adopt various valence states, e.g., $Mo^{IV/V}$ and $W^{IV/V}$. Besides, metal assemblies based on $[M(CN)_8]^{n-}$ can take various dimensional crystal structures, i.e., zero-dimensional (0D),[9] 1D,[10] 2D,[11] and 3D structures.[12] Along this line, we have investigated the photomagnetic properties in new Co-W bimetallic assemblies.[4] Here, we report photoinduced magnetization with a high Curie temperature (T_C) of 48 K and a gigantic coercive field (H_c) of 27 000 Oe in a Co-W bimetal assembly, $[\{Co^{II}(4\text{-methylpyridine})(pyrimidine)\}_2\{Co^{II}(H_2O)_2\}\cdot\{W^V(CN)_8\}_2]\cdot 4H_2O$. These values are the highest reported for photoinduced magnetization systems.

N. Ozaki, Dr. H. Tokoro, Y. Hamada, A. Namai, Dr. T. Matsuda, S. Kaneko, Prof. S. Ohkoshi
Department of Chemistry
School of Science
The University of Tokyo
7-3-1 Hongo, Bunkyo-ku, Tokyo 113-0033, Japan
E-mail: ohkoshi@chem.s.u-tokyo.ac.jp
Dr. H. Tokoro
NEXT, JSPS, 8 Ichibancho, Chiyoda-ku, Tokyo 102-8472, Japan
Prof. S. Ohkoshi
CREST, JST, K's Gobancho
7 Gobancho, Chiyoda-ku, Tokyo 102-0076, Japan

DOI: 10.1002/adfm.201102727

2. Results and Discussion

2.1. Crystal Structure

The target compound was prepared by adding an aqueous solution of $Cs_3[W^V(CN)_8]\cdot 2H_2O$ to a mixed aqueous solution of $Co^{II}Cl_2\cdot 6H_2O$, 4-methylpyridine, and pyrimidine. Elemental analyses confirmed that the formula of the present compound was $[\{Co^{II}(4\text{-methylpyridine})(pyrimidine)\}_2\{Co^{II}(H_2O)_2\}\cdot\{W^V(CN)_8\}_2]\cdot 4H_2O$. The X-ray diffraction (XRD) pattern of the present compound and Rietveld analysis indicated that the present compound had a triclinic crystal structure in the $P\bar{1}$ space group (a = 7.603(4) Å, b = 14.991(6) Å, c = 20.875(10) Å, α = 91.374(4)°, β = 98.32(4)°, γ = 90.65(2)°, and Z = 2; see **Figure 1** and Supporting Information Figure S1,S2 and Table S1). The coordination geometries of the Co (Co1, Co2, Co3, and Co4) sites were pseudo-octahedron (D_{4h}). The equatorial positions of Co1 (or Co2) were occupied by four cyanide nitrogen atoms, whereas the apical positions were occupied by one nitrogen atom of pyrimidine and one nitrogen atom of 4-methylpyridine. Co3 (or Co4) was coordinated with two nitrogen atoms of $[W(CN)_8]$, two oxygen atoms of water molecules, and two nitrogen atoms of pyrimidine. In contrast, W (W1 and W2) sites were dodecahedron (D_{2d}). The five CN groups of W1 (or W2) were bridged to two Co1, two Co2, and one Co4 (or Co3). The other three CN groups were free. This bimetallic assembly had two types of ligand molecules (4-methylpyridine and pyrimidine). 4-methylpyridine coordinated to Co1 or Co2, while the pyrimidine ligand bridged Co1 and Co4 or Co2 and Co3.

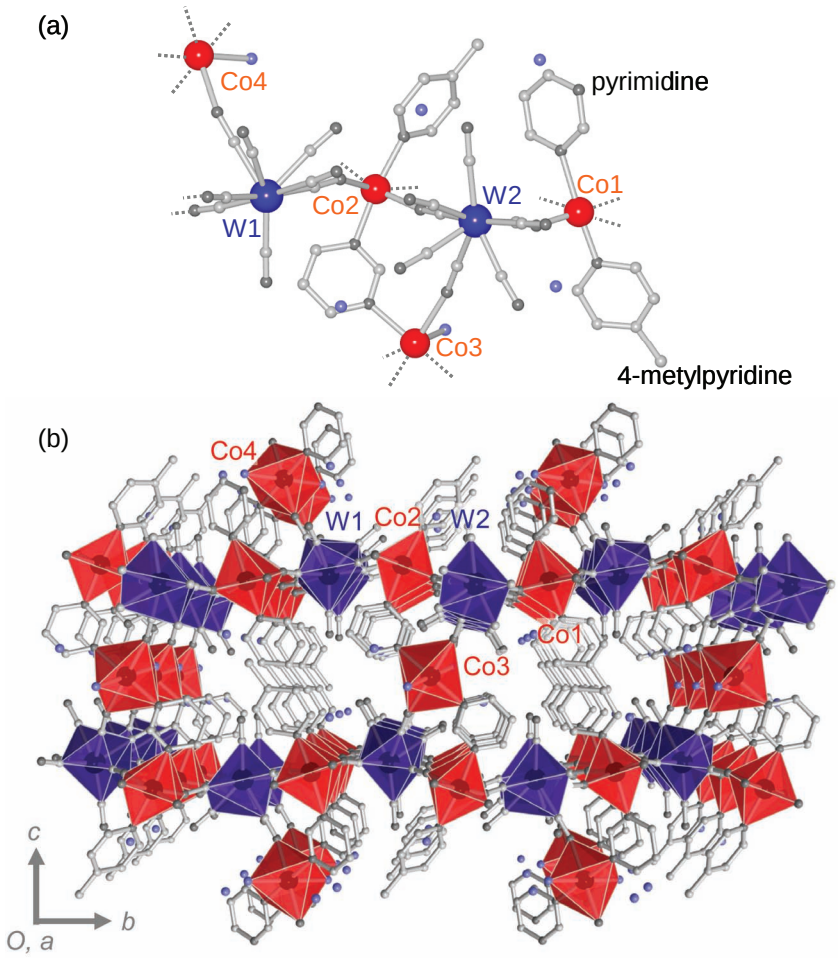

Figure 1. Crystal structure of $[\{Co^{II}(4\text{-methylpyridine})(pyrimidine)\}_2\{Co^{II}(H_2O)_2\}\{W^V(CN)_8\}_2]\cdot 4H_2O$. a) Asymmetric unit. b) View along the *a*-axis. Red, purple, light gray, dark gray, and light purple balls represent Co, W, C, N, and O atoms, respectively. Red and purple polyhedrons represent coordination geometry around Co and W, respectively.

2.2. Thermal Phase Transition

Figure 2 shows the product of the molar magnetic susceptibility (χ_M) and temperature (T) versus T plots. The $\chi_M T$ value at 300 K was 9.23 cm^3 K mol^{-1} (high-temperature (HT) phase), but the value decreased at around 170 K as the sample was cooled at a rate of –1.0 K min^{-1}. At 100 K, the $\chi_M T$ value was 3.27 cm^3 K mol^{-1} (low-temperature (LT) phase) (Supporting Information, Figure S3). Conversely, as the sample was warmed, the $\chi_M T$ value increased at around 240 K, and returned to the initial value at 300 K. The phase transition temperature, which was defined as the temperature where the compound had 50% of the population in the HT and LT phases with decreasing or increasing temperature, was 172 K ($T_{1/2\downarrow}$) or 241 K ($T_{1/2\uparrow}$). The thermal hysteresis ($\Delta T = T_{1/2\uparrow} - T_{1/2\downarrow}$) had a large width of 69 K. In the variable temperature infrared (IR) spectra, as the temperature decreased, an intense broad CN stretching peak appeared around 2150 cm^{-1}, which is assigned to the CN stretching frequency of W^{IV}–C≡N–Co^{III} and W^{IV}–C≡N (Supporting Information, Figure S4). The results of $\chi_M T$–T plots and IR spectroscopy indicate that the observed temperature-induced phase transition from HT phase to LT phase is due to the electronic state change from $Co^{II}_{hs}(S = 3/2)$–$W^V(S = 1/2)$ to $Co^{III}_{ls}(S = 0)$–$W^{IV}(S = 0)$, where *hs* and *ls* denote the high-spin and low-spin states, respectively, i.e., charge-transfer-induced spin transition (CTIST).

Based on the molecular field (MF) theory, the $\chi_M T$ value was fitted using a six-component MF model for $4\text{-}Co^{II}_{(2-4x/3)}4\text{-}Co^{III}_{4x/3}2\text{-}Co^{II}_{(1-2x/3)}2\text{-}Co^{III}_{2x/3}[W^{IV}(CN)_8]_{2x}[W^V(CN)_8]_{(2-2x)}$, where 4-Co and 2-Co represent Co ions coordinated by four cyanide nitrogens (Co1 and Co2) and two cyanide nitrogens (Co3 and Co4), respectively, and x is the transition ratio from the HT phase to the LT phase (see Supporting Information Section 4). The $\chi_M T$–T curve was well reproduced with a g_{Co}-factor of 2.33 by fitting the observed $\chi_M T$ value for the HT phase using a g_W-factor of 1.97 from the electron spin resonance (ESR) spectrum of $Cs_3[W^V(CN)_8]\cdot 2H_2O$ (Supporting Information, Figure S5). In contrast, the $\chi_M T$–T plots with $x = 0.88$ showed the best fit with the observed $\chi_M T$–T plots of the LT phase. Thus, the LT phase was confirmed to have a formula of $(Co^{II}_{hs})_{1.24}(Co^{III}_{ls})_{1.76}[W^{IV}(CN)_8]_{1.76}[W^V(CN)_8]_{0.24}$(4-methylpyridine)$_2$(pyrimidine)$_2\cdot 6H_2O$.

2.3. Photomagnetic Effect

The photomagnetic effect on the LT phase was investigated. The sample was irradiated

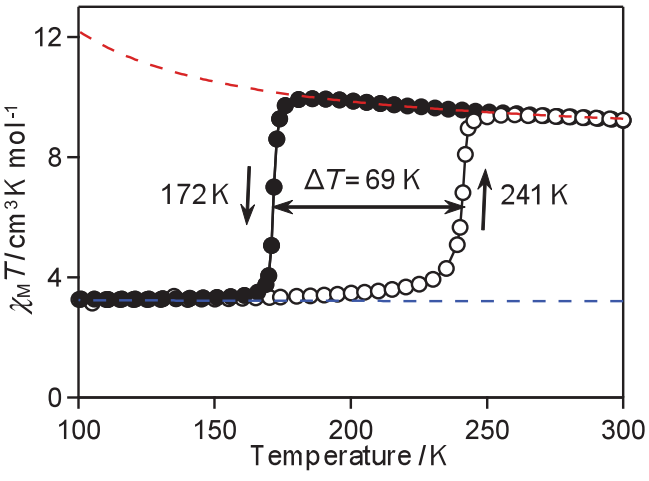

Figure 2. $\chi_M T$–T plots of $[\{Co^{II}(4\text{-methylpyridine})(pyrimidine)\}_2\{Co^{II}(H_2O)_2\}\{W^V(CN)_8\}_2]\cdot 4H_2O$ under 5000 Oe during the cooling (black circles) and warming (white circles) processes. Red and blue dotted lines represent the fitting curves for the HT and LT phases, respectively.

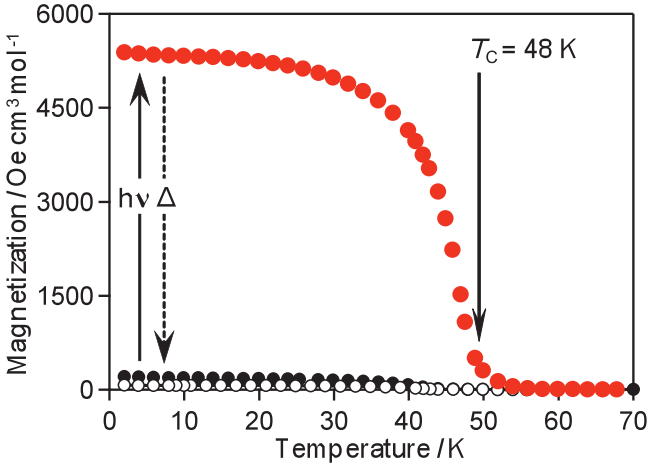

Figure 3. Photoinduced magnetization in [{Co^{II}(4-methylpyridine)(pyrimidine)}$_2$ {$Co^{II}(H_2O)_2$}{$W^V(CN)_8$}$_2$]·4H_2O. FCM curves before irradiation (white circles), after irradiation (red circles), and after thermal treatment (black circles) at 170 K (irradiation conditions: λ = 785 ± 10 nm, 122 mW cm^{-2}, 60 min).

by the 785-nm diode-laser light because the LT phase possesses a metal-to-metal charge transfer (MMCT) band from W^{IV} to Co^{III} in the wavelength region of 600–1000 nm (λ_{max} = 742 nm) (Supporting Information, Figure S6). **Figure 3** shows the field-cooled magnetization (FCM) curves before and after irradiating at 2 K in an external magnetic field of 10 Oe.[13] The irradiated sample exhibited a bulk magnetization with a T_C value of 48 K. Zero-field-cooled magnetization and remanent magnetization curves supported this T_C value (Supporting Information, Figure S7). The magnetization vs. external magnetic field plots after irradiating exhibited a huge magnetic hysteresis loop with a H_c value of 27 000 Oe at 2 K (**Figure 4** and Supporting Information Figure S8) and a saturation magnetization (M_s) value of 8.4 μ_B. Photoinduced magnetization was perfectly maintained for one day below 3 K after the light was turned off, indicating that the photoinduced magnetic phase is persistent. Upon thermal treatment up to 170 K, the photoproduced magnetization value recovered to the initial value (**Figure 5**).

The observed photomagnetic effect can be explained as follows. Irradiating of MM'CT band induces a valence state change from $Co^{III}{}_{ls}$(S = 0)–W^{IV}(S = 0) state to $Co^{II}{}_{ls}$(S = 1/2)–W^V(S = 1/2). Successively, $Co^{II}{}_{ls}$(S = 1/2) changes to the $Co^{II}{}_{hs}$(S = 3/2) state (**Figures 6** and Supporting Information Figure S9), resulting in bulk magnetization. Because the ground Kramers doublet of an octahedral Co^{II} is usually populated, the estimated M_s value for the ferromagnetic ordering is 8.5 μ_B for the given formula,[14] which agrees with the observed value. Hence, the magnetic spins on $Co^{II}{}_{hs}$ and W^V ferromagnetically interact, i.e., superexchange coupling (J_{ex}) between $Co^{II}{}_{hs}$ and W^V through the CN ligand is positive. The large H_c value is attributed to the single-ion magnetic anisotropy of $Co^{II}{}_{hs}$ and magnetocrystalline anisotropy[14,15] due to the character of pseudo 2D crystal structure. One reason the present photomagnetic Co-W system (T_C = 48 K and H_c = 27 000 Oe) is superior to the previous system (T_C = 40 K and H_c = 12 000 Oe)[4a,b] is the distance of Co–NC–W in the *ab*-plane (5.26 Å) is shorter than that in the previous Co-W system (5.36 Å) and this shortened distance

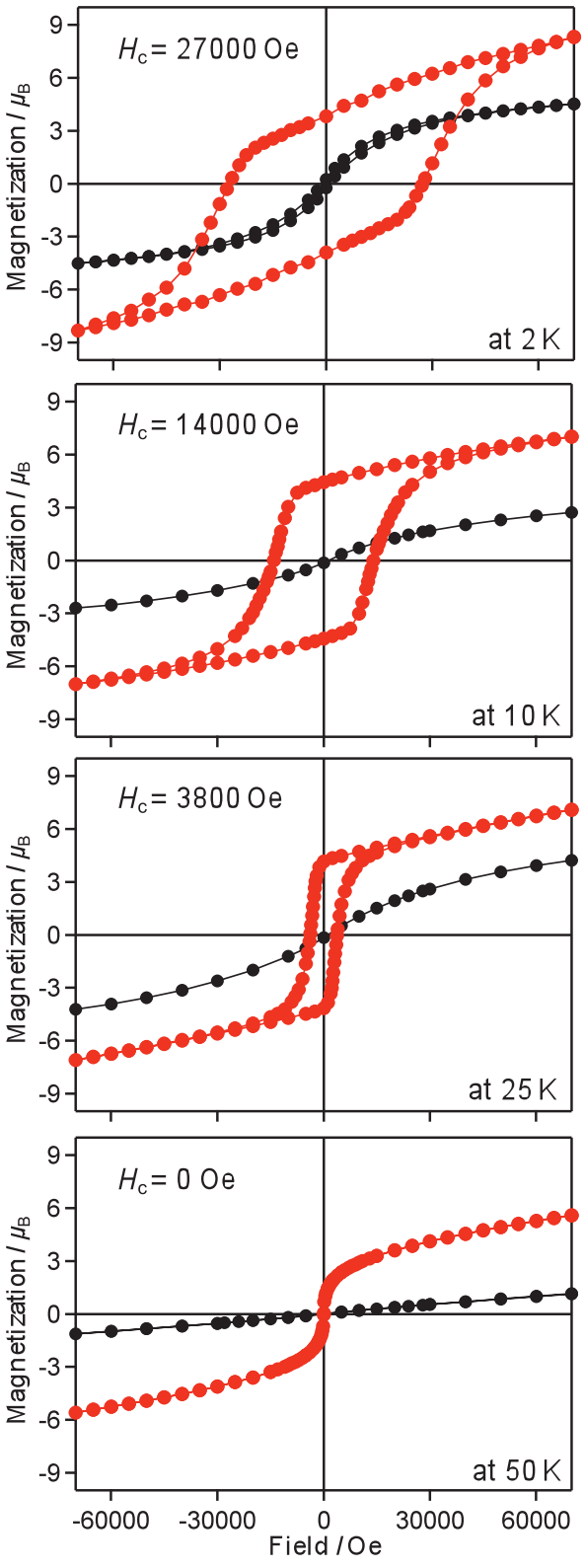

Figure 4. Photoinduced magnetization in [{Co^{II}(4-methylpyridine)(pyrimidine)}$_2$ {$Co^{II}(H_2O)_2$}{$W^V(CN)_8$}$_2$]·4H_2O. Magnetic hysteresis loops at 2 K, 10 K, 25 K, and 50 K after irradiation (red circles) and after thermal treatment (black circles) at 170 K (irradiation conditions: λ = 785 ± 10 nm, 122 mW cm^{-2}, 60 min).

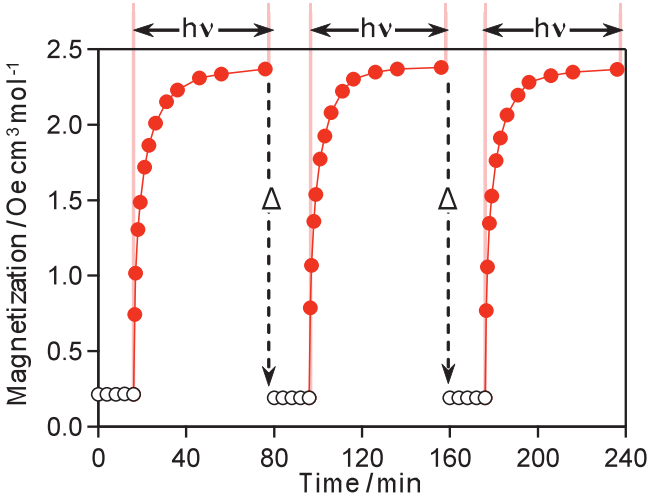

Figure 5. Magnetization vs. irradiation time plots at 2 K under 10 Oe with 785-nm light irradiation (red circles) and after thermal treatment (white circles) at 170 K.

strengthens the superexchange coupling between Co and W in the *ab*-plane. Additionally, the distance between the layers (W–CN–Co–NC–W, 11.5 Å) is longer than that of the previous system (10.9 Å), enhancing the magnetocrystalline anisotropy. Such an improvement is because 4-methylpyridine expands the distance between the layers due to a steric factor.

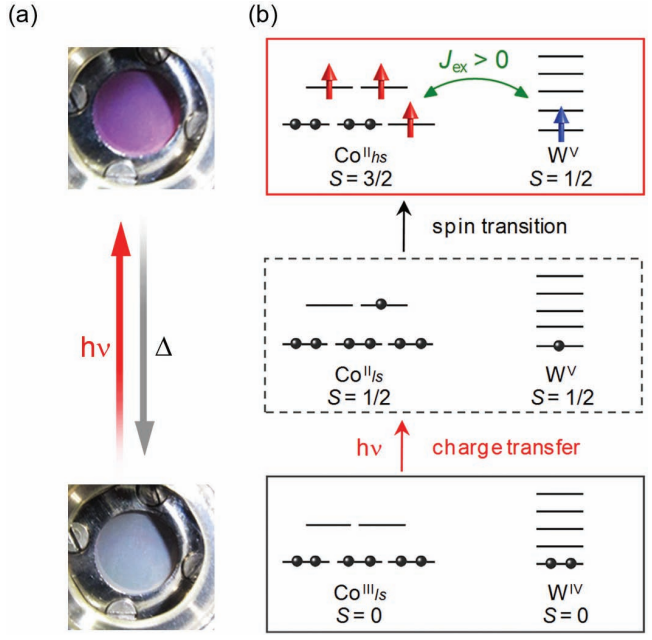

Figure 6. Mechanism of light-induced magnetization in $[\{Co^{II}(4\text{-methylpyridine})(\text{pyrimidine})\}_2\{Co^{II}(H_2O)_2\}\{W^{V}(CN)_8\}_2]\cdot 4H_2O$. a) Photographs of the sample before (lower) and after (upper) the irradiation of 785-nm light at 3 K. b) Schematic illustration of the ferromagnetic ordering due to optically induced charge-transfer-induced spin transition. J_{ex} represents the superexchange coupling between Co^{II}_{hs} and W^{V} through the CN ligand.

3. Conclusions

In conclusion, we prepared a new photomagnet based on a cyanobridged Co-W bimetal assembly, $[\{Co^{II}(4\text{-methylpyridine})(\text{pyrimidine})\}_2\{Co^{II}(H_2O)_2\}\{W^{V}(CN)_8\}_2]\cdot 4H_2O$. The driving force of this photomagnetism is the optically induced CTIST. In the present system, two types of organic molecules (4-methylpyridine and pyrimidine) were used as a coordinating ligand and a bridging ligand, respectively. Thus, combining organic ligand molecules to alter the crystal structure will further improve the photomagnetic properties.

4. Experimental Section

Synthesis: The target compound was prepared by adding a 10 mL aqueous solution of $Cs_3[W^{V}(CN)_8]\cdot 2H_2O$ (1.80 mmol) to a 10 mL mixed aqueous solution of $Co^{II}Cl_2\cdot 6H_2O$ (0.90 mmol), 4-methylpyridine (1.20 mmol), and pyrimidine (1.25 mmol). The mixed solution was stirred for 1 h at 40 °C. The precipitated red powder was filtered, washed with water, and dried in air. Elemental analyses by HP4500 inductively coupled plasma mass spectroscopy and standard microanalytical methods confirmed that the formula of the present compound was $[\{Co^{II}(4\text{-methylpyridine})(\text{pyrimidine})\}_2\{Co^{II}(H_2O)_2\}\{W^{V}(CN)_8\}_2]\cdot 4H_2O$: Calcd: Co 12.50, W 25.99, C 30.53, H 2.40, N 21.77; found: Co 12.47, W 26.28, C 30.48, H 2.31, N 21.94.

Physical Measurements: The magnetic properties were measured by a superconducting quantum interference device (SQUID) magnetometer (Quantum Design, MPMS 7). The IR spectra were recorded with CaF_2 plate using a Shimadzu FTIR-8200PC spectrometer. The ultraviolet-visible (UV-vis) spectra were measured using a Shimadzu UV-3100 spectrometer. The temperature during the optical measurements was controlled by an Oxford Instruments Microstate-He. The XRD measurements were conducted on a Rigaku RINT2100 with Cu Kα radiation ($\lambda = 1.5406$ Å) at 293 K, while Rietveld analysis were performed using RIETAN-FP program [16]. Crystallographic data (excluding structure factors) for the structure reported in this paper have been deposited with the Cambridge Crystallographic Data Centre as supplementary publication no. CCDC-836699. The electron spin resonance (ESR) spectrum was recorded using JEOL JES-FA200. The photomagnetic effect was investigated using a SQUID. The powder sample, spread between a thin glass and a plastic cling film, was placed at the edge of an optical fiber (distance between the fiber and the sample: 8 mm), and a continuous wave (cw) diode laser of 785 ± 10 nm was used as a light source (122 mW cm^{-2}).

Supporting Information

Supporting Information is available from the Wiley Online Library or from the author.

Acknowledgements

The authors are grateful to Y. Tsunobuchi (the University of Tokyo) for the experimental support. The present research was supported in part by the CREST program of JST, a Grant-in-Aid for Young Scientists (S) and the NEXT program from JSPS, the Global COE Program "Chemistry Innovation through Cooperation of Science and Engineering", the Photon Frontier Network Program from MEXT, Sekisui Integrated Research, the Izumi foundation, and the Asahi Glass foundation.

Received: November 12, 2011
Revised: January 12, 2012
Published online: March 1, 2012

[1] a) S. Ferlay, T. Mallah, R. Ouahès, P. Veillet, M. Verdaguer, *Nature* **1995**, *378*, 701; b) S. M. Holmes, G. S. Girolami, *J. Am. Chem. Soc.* **1999**, *121*, 5593; c) Ø. Hatlevik, W. E. Buschmann, J. Zhang, J. L. Manson, J. S. Miller, *Adv. Mater.* **1999**, *11*, 914; d) S. Ohkoshi, M. Mizuno, G. J. Hung, K. Hashimoto, *J. Phys. Chem. B* **2000**, *104*, 9365.

[2] a) Y. Zhang, D. Li, R. Clérac, M. Kalisz, C. Mathonière, S. M. Holmes, *Angew. Chem. Int. Ed.* **2010**, *49*, 3752; b) M. G. Hilfiger, M. Chen, T. V. Brinzari, T. M. Nocera, M. Shatruk, D. T. Petasis, J. J. Musfeldt, C. Achim, K. R. Dunbar, *Angew. Chem. Int. Ed.* **2010**, *49*, 1410; c) H. Tokoro, S. Ohkoshi, T. Matsuda, K. Hashimoto, *Inorg. Chem.* **2004**, *43*, 5231; d) A. Bleuzen, V. Escax, A. Ferrier, F. Villain, M. Verdaguer, P. Münsch, J. P. Itié, *Angew. Chem. Int. Ed.* **2004**, *43*, 3728; e) N. Shimamoto, S. Ohkoshi, O. Sato, K. Hashimoto, *Inorg. Chem.* **2002**, *41*, 678.

[3] a) S. Ohkoshi, K. Imoto, Y. Tsunobuchi, S. Takano, H. Tokoro, *Nat. Chem.* **2011**, *3*, 564; b) D. M. Pajerowski, M. J. Andrus, J. E. Gardner, E. S. Knowles, M. W. Meisel, D. R. Talham, *J. Am. Chem. Soc.* **2010**, *132*, 4058; c) H. Tokoro, T. Matsuda, T. Nuida, Y. Moritomo, K. Ohoyama, E. D. Loutete-Dangui, K. Boukheddaden, S. Ohkoshi, *Chem. Mater.* **2008**, *20*, 423; d) J. W. Yoo, R. S. Edelstein, D. M. Lincoln, N. P. Raju, A. J. Epstein, *Phys. Rev. Lett.* **2007**, *99*, 157205; e) S. Ohkoshi, H. Tokoro, T. Hozumi, Y. Zhang, K. Hashimoto, C. Mathonière, I. Bord, G. Rombaut, M. Verelst, C. C. dit Moulin, F. Villain, *J. Am. Chem. Soc.* **2006**, *128*, 270; f) A. Bleuzen, C. Lomenech, V. Escax, F. Villain, F. Varret, C. C. dit Moulin, M. Verdaguer, *J. Am. Chem. Soc.* **2000**, *122*, 6648; g) S. Ohkoshi, S. Yorozu, O. Sato, T. Iyoda, A. Fujishima, K. Hashimoto, *Appl. Phys. Lett.* **1997**, *70*, 1040; h) O. Sato, T. Iyoda, A. Fujishima, K. Hashimoto, *Science* **1996**, *272*, 704.

[4] a) S. Ohkoshi, S. Ikeda, T. Hozumi, T. Kashiwagi, K. Hashimoto, *J. Am. Chem. Soc.* **2006**, *128*, 5320; b) S. Ohkoshi, Y. Hamada, T. Matsuda, Y. Tsunobuchi, H. Tokoro, *Chem. Mater.* **2008**, *20*, 3048; c) R. Le Bris, C. Mathonière, J. F. Létard, *Chem. Phys. Lett.* **2006**, *426*, 380; d) Y. Arimoto, S. Ohkoshi, Z. Zhong, H. Seino, Y. Mizobe, K. Hashimoto, *J. Am. Chem. Soc.* **2003**, *125*, 9240.

[5] a) S. Ohkoshi, K. Arai, Y. Sato, K. Hashimoto, *Nat. Mater.* **2004**, *3*, 857; b) N. Yanai, W. Kaneko, K. Yoneda, M. Ohba, S. Kitagawa, *J. Am. Chem. Soc.* **2007**, *129*, 3496; c) J. Milon, M. Daniel, A. Kaiba, P. Guionneau, S. Brandès, J. P. Sutter, *J. Am. Chem. Soc.* **2007**, *129*, 13872.

[6] a) C. Train, T. Nuida, R. Gheorghe, M. Gruselle, S. Ohkoshi, *J. Am. Chem. Soc.* **2009**, *131*, 16838; b) T. Nuida, T. Matsuda, H. Tokoro, S. Sakurai, K. Hashimoto, S. Ohkoshi, *J. Am. Chem. Soc.* **2005**, *127*, 11604; c) K. Ikeda, S. Ohkoshi, K. Hashimoto, *J. Appl. Phys.* **2003**, *93*, 1371.

[7] a) S. S. Kaye, H. J. Choi, J. R. Long, *J. Am. Chem. Soc.* **2008**, *130*, 16921; b) S. Ohkoshi, Y. Tsunobuchi, H. Takahashi, T. Hozumi, M. Shiro, K. Hashimoto, *J. Am. Chem. Soc.* **2007**, *129*, 3084.

[8] a) A. L. Goodwin, M. Calleja, M. J. Conterio, M. T. Dove, J. S. O. Evans, D. A. Keen, L. Peters, M. G. Tucker, *Science* **2008**, *319*, 794; b) K. W. Chapman, P. J. Chupas, C. J. Kepert, *J. Am. Chem. Soc.* **2006**, *128*, 7009; c) S. Margadonna, K. Prassides, A. N. Fitch, *J. Am. Chem. Soc.* **2004**, *126*, 15390.

[9] a) Z. J. Zhong, H. Seino, Y. Mizobe, M. Hidai, A. Fujishima, S. Ohkoshi, K. Hashimoto, *J. Am. Chem. Soc.* **2000**, *122*, 2952; b) J. Larionova, M. Gross, M. Pilkington, H. Andres, H. S. Evans, H. U. Güdel, S. Decurtins, *Angew. Chem. Int. Ed.* **2000**, *39*, 1605; c) B. Sieklucka, J. Szklarzewicz, *Inorg. Chem.* **2000**, *39*, 5156; d) F. Bonadio, M. Gross, H. S. Evans, S. Decurtins, *Inorg. Chem.* **2002**, *41*, 5891; e) J. M. Herrera, V. Marvaud, M. Verdaguer, J. Marrot, M. Kalisz, C. Mathonière, *Angew. Chem. Int. Ed.* **2004**, *43*, 5468; f) D. E. Freedman, M. V. Bennett, J. R. Long, *Dalton Trans.* **2006**, *23*, 2829; g) J. H. Lim, J. H. Yoon, H. C. Kim, C. S. Hong, *Angew. Chem. Int. Ed.* **2006**, *45*, 7424.

[10] a) G. Rombaut, S. Golhen, L. Ouahab, C. Mathonière, O. Kahn, *J. Chem. Soc. Dalton Trans.* **2000**, *20*, 3609; b) R. Podgajny, T. Korzeniak, K. Stadnicka, Y. Dromzée, N. W. Alcock, W. Errington, K. Kruczała, M. Balanda, T. J. Kemp, M. Verdaguer, B. Sieklucka, *Dalton Trans.* **2003**, *17*, 3458; c) R. Pradhan, C. Desplanches, P. Guionneau, J. P. Sutter, *Inorg. Chem.* **2003**, *42*, 6607; d) S. Ikeda, T. Hozumi, K. Hashimoto, S. Ohkoshi, *Dalton Trans.* **2005**, *12*, 2120; e) F. Prins, E. Pasca, L. J. Jongh, H. Kooijman, A. L. Spek, S. Tanase, *Angew. Chem. Int. Ed.* **2007**, *46*, 6081; f) T. S. Venkatakrishnan, S. Sahoo, N. Bréfuel, C. Duhayon, C. Paulsen, A. L. Barra, S. Ramasesha, J. P. Sutter, *J. Am. Chem. Soc.* **2010**, *132*, 6047.

[11] a) T. Korzeniak, K. Stadnicka, M. Rams, B. Sieklucka, *Inorg. Chem.* **2004**, *43*, 4811; b) S. Ohkoshi, Y. Arimoto, T. Hozumi, H. Seino, Y. Mizobe, K. Hashimoto, *Chem. Commun.* **2003**, *22*, 2772.

[12] a) R. Garde, C. Desplanches, A. Bleuzen, P. Veillet, M. Verdaguer, *Mol. Cryst. Liq. Cryst.* **1999**, *334*, 587; b) Z. J. Zhong, H. Seino, Y. Mizobe, M. Hidai, M. Verdaguer, S. Ohkoshi, K. Hashimoto, *Inorg. Chem.* **2000**, *39*, 5095; c) T. Kashiwagi, S. Ohkoshi, H. Seino, Y. Mizobe, K. Hashimoto, *J. Am. Chem. Soc.* **2004**, *126*, 5024; d) J. M. Herrera, P. Franz, R. Podgajny, M. Pilkington, M. Biner, S. Decurtins, H. S. Evans, A. Neels, R. Garde, Y. Dromzée, M. Julve, B. Sieklucka, K. Hashimoto, S. Ohkoshi, M. Verdaguer, *C. R. Chimie* **2008**, *11*, 1192.

[13] Before irradiation, a small magnetization, which is due to the remained HT state, was observed. The observed LT phase is composed of $[Co^{II}_{hs}(S = 3/2)]_{1.24}$–$[W^{V}(S = 1/2)]_{0.24}$–$[Co^{III}_{ls}(S = 0)]_{1.76}$–$[W^{IV}(S = 0)]_{1.76}$, i.e., the thermal phase transition ratio from HT phase to LT phase is 88%. 12% of the W ions can connect $Co^{II}_{hs}(S = 3/2)$ and then a spin percolation may exist. This spin network (or spin cluster) is considered to produce a small magnetization (ca. 2% compared to the photoinduced magnetization). When the thermal phase transition from HT phase to LT phase undergoes completely, such a small magnetization should not appear.

[14] a) R. L. Carlin, *Magnetochemistry*, Springer-Verlag, Berlin **1986**; b) L. Banci, A. Bencini, C. Benelli, D. Gatteschi, C. Zanchini, *Struct. Bonding (Berlin)* **1982**, *52*, 37.

[15] S. Chikazumi, *Physics of Ferromagnetism 2nd ed.*, Oxford University Press, New York **1997**.

[16] F. Izumi, K. Momma. *Solid. State. Phenom.* **2007**, *130*, 15.